

THE ORIGIN OF ASTEROID 162173 (1999 JU₃)

HUMBERTO CAMPINS¹, JULIA DE LEÓN^{2,3}, ALESSANDRO MORBIDELLI⁴, JAVIER LICANDRO^{5,6},
JULIE GAYON-MARKT⁴, MARCO DELBO⁴, AND PATRICK MICHEL⁴

¹ Physics Department, University of Central Florida, P.O. Box 162385, Orlando, FL 32816-2385, USA

² Department of Edaphology and Geology, University of La Laguna, E-38071 Tenerife, Spain

³ Instituto de Astrofísica de Andalucía-CSIC, Camino Bajo de Huétor 50, E-18008 Granada, Spain

⁴ Observatoire de la Côte d'Azur, Université de Nice Sophia Antipolis (UNS), CNRS UMR7293, F-06108 Nice Cedex 2, France

⁵ Instituto de Astrofísica de Canarias (IAC), C/Vía Láctea s/n, E-38205 La Laguna, Spain

⁶ Department of Astrophysics, University of La Laguna, E-38205 La Laguna, Tenerife, Spain

Received 2012 June 27; accepted 2013 April 30; published 2013 July 11

ABSTRACT

Near-Earth asteroid (162173) 1999 JU₃ (henceforth JU₃) is a potentially hazardous asteroid and the target of the Japanese Aerospace Exploration Agency's Hayabusa-2 sample return mission. JU₃ is also a backup target for two other sample return missions: NASA's OSIRIS-REx and the European Space Agency's Marco Polo-R. We use dynamical information to identify an inner-belt, low-inclination origin through the ν_6 resonance, more specifically, the region with $2.15 \text{ AU} < a < 2.5 \text{ AU}$ and $i < 8^\circ$. The geometric albedo of JU₃ is 0.07 ± 0.01 , and this inner-belt region contains four well-defined low-albedo asteroid families (Clarissa, Erigone, Polana, and Sulamitis), plus a recently identified background population of low-albedo asteroids outside these families. Only two of these five groups, the background and the Polana family, deliver JU₃-sized asteroids to the ν_6 resonance, and the background delivers significantly more JU₃-sized asteroids. The available spectral evidence is also diagnostic; the visible and near-infrared spectra of JU₃ indicate it is a C-type asteroid, which is compatible with members of the background, but not with the Polana family because it contains primarily B-type asteroids. Hence, this background population of low-albedo asteroids is the most likely source of JU₃.

Key words: minor planets, asteroids: general – minor planets, asteroids: individual (162173, 1999 JU₃)

Online-only material: color figures

1. INTRODUCTION

Near-Earth asteroid (162173) 1999 JU₃ (henceforth JU₃) is the primary target of the Japanese Aerospace Exploration Agency (JAXA) Hayabusa-2 sample return mission with a planned launch in 2014. This object is also in the list of potential targets for two other sample return missions: NASA's OSIRIS-REx, selected in 2011 as the next New Frontiers mission, and the European Space Agency (ESA) Marco Polo-R mission, selected in 2011 for the assessment study phase of ESA's M3 missions.

These space missions seek to understand the origin and nature of volatile and organic material in the early solar system; hence, samples of a primitive asteroid (B, C, D, F, and P asteroids in the Tholen classification system; Tholen & Barucci 1989) are highly desirable. JU₃ has been classified as a Cg-type (Binzel et al. 2001) in the Small Main-Belt Asteroid Spectroscopic Survey classification system (SMASS; Bus & Binzel 2002a, 2002b). This classification is within the C-class in the Tholen system. C-class objects are present in the inner belt (within 2.5 AU) but are most abundant in the middle to the outer main belt; they are believed to be primitive, volatile-rich remnants from the early solar system.

JU₃ has a quasi-spherical shape, with visible geometric albedo $p_v = 0.07 \pm 0.01$, diameter $= 0.87 \pm 0.03 \text{ km}$, and thermal inertia between 200 and 600 $\text{Jm}^{-2} \text{s}^{-0.5} \text{K}^{-1}$. The latest thermal models (Müller et al. 2011) incorporate estimates of the shape and spin–vector orientation for this asteroid; however, all published estimates of these three quantities are in agreement within the uncertainties (Hasegawa et al. 2008; Campins et al. 2009; Müller et al. 2011). The maximum estimated value of the thermal inertia for JU₃ is lower than the 750 $\text{Jm}^{-2} \text{s}^{-0.5} \text{K}^{-1}$ for asteroid 25143 Itokawa (Fujiwara et al. 2006).

In this work, we combine dynamical, albedo, and spectral information to identify the most likely main belt origin of JU₃. We use a similar approach to that of Campins et al. (2010) and de León et al. (2010a) and we conclude that a background population of low-albedo inner-belt asteroids is the most likely source of JU₃.

2. DYNAMICAL AND PHYSICAL CONSTRAINTS

In this section, we start with the orbital dynamics, which quickly restrict the likely source region of JU₃ to the inner belt with inclinations lower than 8° . The albedo of JU₃ further restricts the potential sources within this region to four low-albedo families, and a newly identified background population of low-albedo asteroids outside these families (Gayon-Markt et al. 2012). Additional considerations, such as location, size distribution, and spectral characteristics favor the background population.

2.1. Likely Origin of the Current Orbit

The orbital elements of JU₃ are given in Table 1; based on this orbit, it is possible to constrain the region of the main belt where it originated. A method for estimating the origin of Near Earth Objects (NEOs) is described in Bottke et al. (2002). More specifically, they numerically integrated the orbits of thousands of test particles, starting from the five most efficient source regions of NEOs. These source regions are (1) the ν_6 secular resonance at $\sim 2.15 \text{ AU}$, which marks the inner border of the main belt; (2) the Mars-crossing asteroid population, adjacent to the main belt; (3) the 3:1 mean-motion resonance with Jupiter at 2.5 AU; (4) the outer main-belt population between 2.8 and 3.5 AU; and (5) the Jupiter-family comets. According to this model for NEO sources, the orbit of JU₃ has a

Table 1Osculating Orbital Elements of JU₃ at Epoch 2455800.5 (2011 Aug 27.0)^a

Aphelion distance	1.4161 AU
Perihelion distance	0.9633 AU
Semi-major axis	1.1897 AU
Eccentricity	0.1903
Orbital period	1.30 yr
Mean anomaly	282.72°
Inclination	5.88°
Longitude of ascending node	251.62°
Argument of perihelion	211.42°

Note. ^a From NASA’s Jet Propulsion Laboratory (<http://ssd.jpl.nasa.gov>).

~80% probability to have been reached by objects that escaped through the ν_6 resonance, a ~20% probability through the Mars-crossing asteroid population, and a negligible chance to have originated from the 3:1 mean-motion resonance with Jupiter or further away from the Sun, including Jupiter-family comets.⁷ Furthermore, all ν_6 source orbits have initial inclinations lower than 12° and 90% of them lower than 8°. The ν_6 secular resonance does not have a strong effect on the inclination of the asteroids that enter it. However, these asteroids have their orbital eccentricities increased to values that can render them Earth-crossers (Bottke et al. 2002).

In principle, the Mars-crossing asteroid population can originate from anywhere inward of 2.8 AU (Bottke et al. 2002). However, the simulations in Bottke et al. (2002) show that none of the Mars-crossing objects that originate beyond 2.5 AU reach the JU₃ orbit, so we consider the 20% probability of a Mars-crossing source to also be originally from the inner belt. These dynamical arguments constrain strongly the most likely source region to orbits between 2.15 and 2.5 AU and with inclinations lower than 8°.

2.2. Retrograde Rotation

In order for the Yarkovsky effect to move objects from the inner-belt region into the ν_6 resonance by decreasing the semi-major axis, their rotation has to be retrograde, as is the case of JU₃ (Müller et al. 2011). However, the spin axis of this asteroid could have changed either due to small impacts while the object was in the main belt or due to the YORP effect. So, although the current spin state of JU₃ does not necessarily constrain what it was when it formed, its current spin axis orientation is consistent with an inward orbital evolution into the ν_6 resonance.

2.3. Low Albedo

The geometric albedo for JU₃ is $p_v = 0.07 \pm 0.01$ (Müller et al. 2011; Campins et al. 2009; Hasegawa et al. 2008). The low-inclination inner belt contains four low-albedo asteroid families (defined here as geometric albedo <8%). These are the Clarissa, Erigone, Polana,⁸ and Sulamitis families (Figure 1(a)). The average geometric albedo of these three families is 0.059 ± 0.025 for Clarissa asteroids, 0.054 ± 0.013 for Erigone asteroids,

0.057 ± 0.015 for Polana asteroids, and 0.056 ± 0.013 for Sulamitis asteroids, based on NASA’s *Wide-Field Infrared Survey Explorer* (WISE) observations (Masiero et al. 2011). In addition, this region contains a recently identified group of primitive asteroids (Gayon-Markt et al. 2012; Walsh et al. 2013), not contained within these four families. Although this group was identified by its Sloan Digital Sky Survey (SDSS; Parker et al. 2008) colors, asteroids with primitive colors or spectra (B, C, and P asteroids in the Tholen classification system) also have low albedos measured by NASA’s WISE (Mainzer et al. 2011). Hence, we refer to this background group as the low-albedo and low-inclination background, and in Figure 1(b) we use the WISE observations to show its structure.

2.4. Source Location and Contribution to the ν_6 Resonance

Small asteroids like JU₃ (diameter ~1 km) are unlikely to be primordial objects because their collisional lifetime is much shorter than the age of the solar system (Bottke et al. 2005). Thus, JU₃ must be a fragment of a larger object. Asteroid families and any collisionally evolved population of asteroids will yield small fragments in the size of JU₃, either during the family-forming event (a catastrophic disruption of a large asteroid tens to hundreds of kilometers in size) or during the collisional evolution that normally occurs in the asteroid belt.

Of the five possible source populations mentioned in Section 2.3, the low-albedo and low-inclination background is closest to the ν_6 resonance; in fact, the inner edge of this population is this resonance (Figure 1(b)). Hence, this background population has been and is currently delivering asteroids to the ν_6 resonance, with many of these asteroids large enough (~1 km diameter) to produce JU₃. In fact, the background population contains more kilometer-sized objects than each of the four families. More specifically, the observed size distribution of the background population allows us to obtain an estimate of the abundance of kilometer-sized objects in it using Gayon-Markt et al. (2012, their Figure 5). Although the absolute magnitudes in Gayon-Markt et al. are complete only to about $H_v = 15$ (diameter of about 5 km assuming a 5% albedo), all plausible extrapolations yield a number of kilometer-sized background asteroids roughly twice those of the Polana family. A similar analysis for the other three families yields even greater ratios of kilometer-sized background to Erigone, Sulamitis, and Clarissa objects, respectively. Hence, the abundance of kilometer-sized objects favors background asteroids over each of these four families.

Since the cores of the four families are further from the ν_6 resonance than the background group of asteroids, it is important to estimate the ability of these families to deliver objects the size of JU₃ to the ν_6 resonance. Dynamical arguments show that the Polana family has already delivered objects with diameters of 1 km (and smaller) to the ν_6 resonance; this evidence has been described in Campins et al. (2010), so we will not go into details here. However, other factors make this family an unlikely source for JU₃; as we discuss in the next section, the colors and spectra of Polana family members are different from those for JU₃. In the other three families, the dynamics do not favor the delivery of objects the size of JU₃ to the ν_6 resonance. More specifically, the absolute magnitude (H_v) versus proper semi-major axis plot is used to estimate the size of the family members that reach the ν_6 resonance. Starting with the Erigone family (Figure 2 (upper panel)), we see the characteristic “V”-shape, a feature known to be associated both with the size-dependent ejection velocity field, as well as with the drift in

⁷ Our probabilities differ slightly from those used in Michel & Delbo (2010), principally because they divided the origin of the Mars-crossing source roughly equally between the ν_6 and the 3:1 resonances. As discussed above, in the case of JU₃ the Mars-crossing source is entirely from within 2.5 AU.

⁸ Here we call the Polana family the low-albedo component of the Nysa–Polana complex. Polana members can also be identified by their visible colors or spectra (e.g., Gayon-Markt et al. 2012; Campins et al. 2010; Cellino et al. 2001).

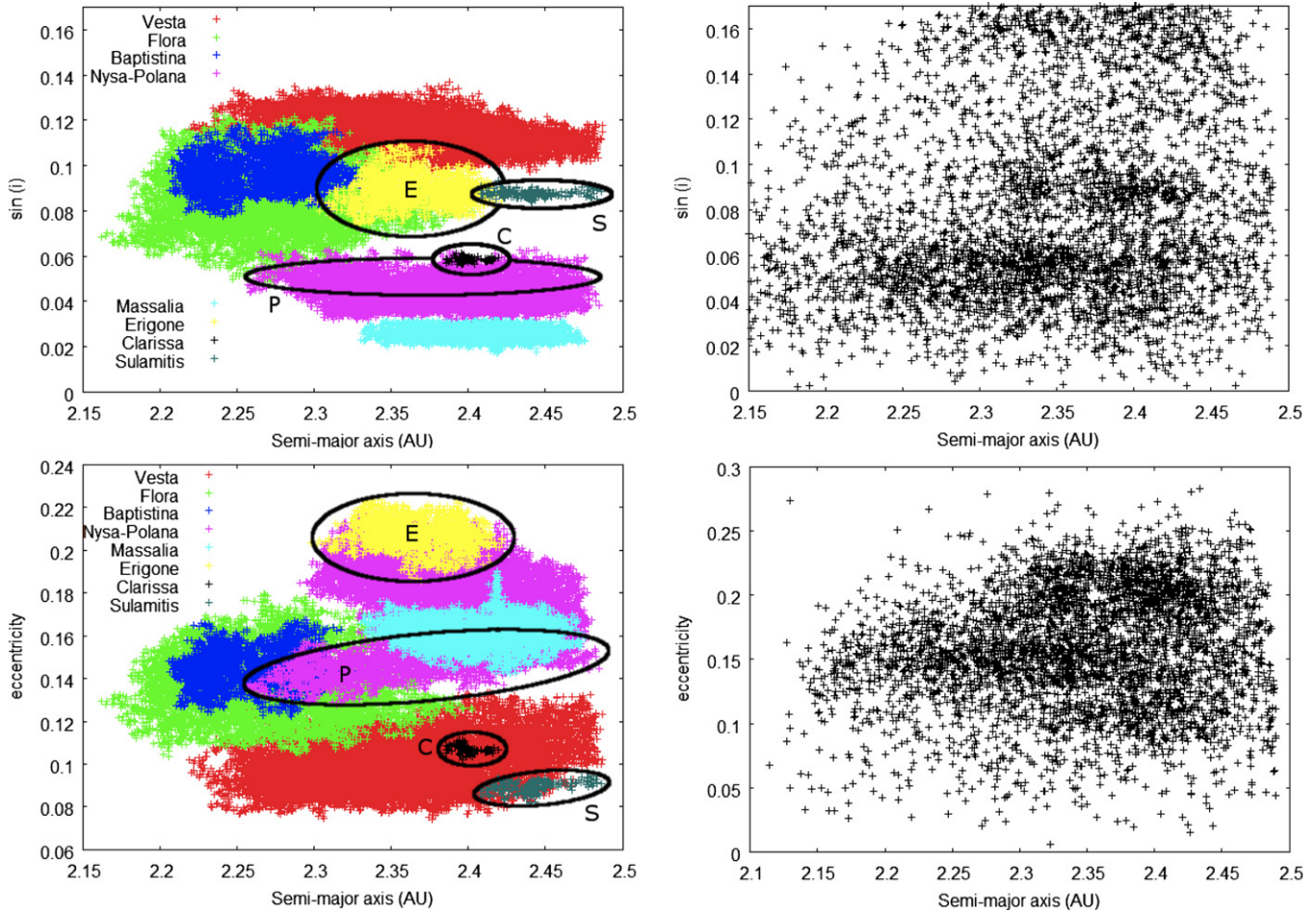


Figure 1. (a) Inner-belt low-inclination ($i < 10^\circ$, $\sin i < 0.17^\circ$) families according to Nesvorný (2010). Highlighted by the black ovals are the four low-albedo ($p_v < 8\%$) and low-inclination families, namely Clarissa, Erigone, Polana, and Sulamitis. The Polana family is part of the Nysa–Polana complex and Polana members can be differentiated by their Sloan Digital Sky Survey (SDSS) colors (e.g., Campins et al. 2010; Gayon-Markt et al. 2012) and by their low albedo. (b) The same inner-belt low-inclination region showing *WISE* observations of low-albedo background asteroids (Masiero et al. 2011) outside the families. This panel illustrates how the background extends to the ν_6 resonance and, as the text explains, is the most likely source of JU_3 . Note that this background shows “halos” around low-albedo families, most prominently around the Polana and Erigone families. These halos contain asteroids that do not meet the dynamical criteria for family membership, but are clearly related to those families. There is also a concentration of background objects near the top of panel (b) not associated with any family identified in Nesvorný (2010).

(A color version of this figure is available in the online journal.)

the proper semi-major axis “ a_p ” induced by the Yarkovsky effect⁹ (e.g., Vokrouhlický et al. 2006). The dashed curves in the figure show the H -dependent semi-major axis distribution induced by the Yarkovsky effect that best fit the boundaries of the observed distribution. Bodies below these curves are expected to be interlopers, i.e., not genetically linked to this family, or ejected with a sufficiently large initial velocity to have reached a significantly larger distance from the original semi-major axis. As expected, objects in these plots extend to both sides of the family’s main fragment.

In the direction of shorter semi-major axes¹⁰, the extrapolated Yarkovsky-induced distribution for the Erigone family predicts

⁹ We also note that the core of the family (the center of the “V”) will contain some objects that drifted due to the Yarkovsky effect toward the center after the family formed; i.e., objects with prograde rotation that drifted from smaller semi-major axes and retrograde rotators that drifted the opposite way.

¹⁰ The apparent edge of Erigone family members short of ~ 2.32 AU is at least in part due to an observational bias against objects too faint to be properly observed by current surveys. In addition, the 5:4:1 Jupiter–Saturn–asteroid resonance (Morbidelli & Nesvorný 1999) also at ~ 2.32 AU could contribute to a depletion of Erigone family objects drifting inward; as mentioned in the main text, although this resonance can also deliver objects to near-Earth orbits, its efficiency is much lower than that of the ν_6 resonance.

that objects with magnitude $H_v \sim 20.2$ should reach the outer edge of the ν_6 resonance (at ~ 2.15 AU for the inclination of 5° characteristic of this family; Morbidelli & Gladman 1998). For an Erigone-like albedo of $p_v = 5.4\%$, this absolute magnitude translates into a diameter $D = 0.5 \pm 0.05$ km, i.e., about half that of JU_3 (the uncertainties in fitting the Yarkovsky curves are approximately 20% in magnitude, which translate into diameter estimate uncertainties of 10%). Thus, no JU_3 -sized Erigone family fragments have reached near-Earth orbits through the ν_6 resonance yet. There are other resonances between the core of the Erigone family and the ν_6 resonance that could deliver objects to near-Earth space, albeit with much lower efficiencies than the ν_6 resonance. For example, the 7:2 with Jupiter at 2.25 AU and the 5:4:1 three-body resonance Jupiter–Saturn–asteroid at 2.32 AU could deliver objects (Morbidelli & Nesvorný 1999); thus, JU_3 -sized Erigone family fragments may have reached near-Earth orbits through these resonances. However, the background population is also contributing to these resonances, and in larger numbers, so the background asteroids seem to always dominate the Erigone family as a likely source of JU_3 .

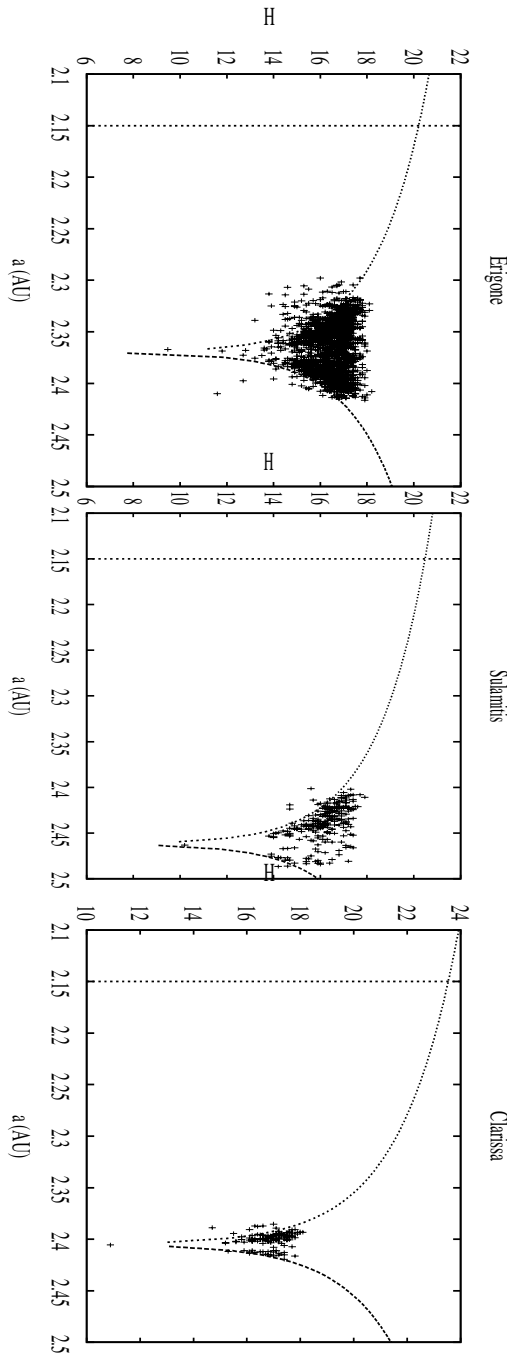


Figure 2. Upper panel: the absolute magnitude (H_v) vs. proper semi-major axis (a) plot for the Erigone family. The dashed lines show the H_v -dependent semi-major axis distribution induced by the Yarkovsky effect that best fit the boundaries of the observed distribution. Bodies below these curves are expected to be interlopers, i.e., not genetically linked to this family. The extrapolated Yarkovsky-induced distribution predicts that members of this family enter the ν_6 resonance when they reach values of their semi-major axis “ a ” of 2.15 AU (vertical line at 2.15 AU for the inclination of 5° characteristic of this family; Morbidelli & Gladman 1998), which happens for objects with absolute magnitude $H_v = 20.2$. This absolute magnitude for an Erigone-like albedo of $p_v = 5.4\%$, translates into a diameter $D = 0.5 \pm 0.05$ km, i.e., about half the size of JU₃. Middle panel: the same plot for the Sulamitis family indicates that objects with $H_v = 20.5$ reach the ν_6 resonance. For a Sulamitis-like albedo of $p_v = 5.6\%$, this absolute magnitude translates into a diameter $D = 0.4 \pm 0.04$ km. Objects do not extend as far on the right side of the middle panel because they encounter the 3:1 mean-motion resonance with Jupiter near 2.5 AU. Lower panel: the same plot for the Clarissa family indicates that objects with $H_v = 23.6$ reach the ν_6 resonance, which for a Clarissa-like albedo of $p_v = 5.9\%$, this absolute magnitude translates into a diameter $D = 0.02 \pm 0.002$ km, much smaller than that of JU₃.

Similar arguments indicate that the Clarissa and Sulamitis families do not extend sufficiently toward the ν_6 resonance to deliver an object the size of JU₃. More specifically, the Yarkovsky-induced distribution for the Sulamitis family (Figure 2, middle panel) predicts that it should reach the outer edge of the ν_6 resonance (at ~ 2.15 AU for the inclination of 5° characteristic of this family; Morbidelli & Gladman 1998) for objects with $H_v = 20.5$. For a Sulamitis-like albedo of $p_v = 5.6\%$, this magnitude translates into a diameter $D = 0.4 \pm 0.04$ km, again significantly smaller than that of JU₃. The Sulamitis family appears to be an important source of asteroids to the 3:1 resonance, but not to the ν_6 resonance. Since the Bottke et al. (2002) model rules out transport via the 3:1 resonance for the origin of JU₃’s current orbit, we do not favor the Sulamitis family as a likely source. For the Clarissa family (Figure 2, lower panel), objects with $H_v = 23.6$ reach the ν_6 resonance, which for a Clarissa-like albedo of $p_v = 5.9\%$, this magnitude translates into a diameter $D = 0.02 \pm 0.002$ km.

In summary, location and size distribution favor the low-albedo and low-inclination background over the four low-albedo inner-belt families, as the most likely source of JU₃.

2.5. Spectral Comparisons

We now consider the spectral information available on JU₃ and on the candidate sources. The available spectral evidence is nicely complementary to the dynamical and albedo constraints because it rules out one of the two remaining candidate populations, the Polana family, and is consistent with the background. Figure 3 shows three different spectra of JU₃ at visible wavelengths (0.4–1.0 μm ; Binzel et al. 2001; Abe et al. 2008; Vilas 2008), and one near-infrared spectrum (0.8–2.4 μm ; Abe et al. 2008). A more recent near-infrared spectrum (Pinilla-Alonso et al. 2013) is essentially identical to that in Abe et al. (2008), but the newer spectrum has lower signal-to-noise because the asteroid was fainter. We note that the three visible spectra are not entirely consistent with each other. For several reasons, we use the visible spectrum with highest signal-to-noise, which was obtained in 2007 September (Vilas 2008). This is the visible spectrum with the best 0.8–0.9 μm overlap with the near-infrared spectrum (Figure 3) and is essentially identical to three new spectra of JU₃ obtained during its 2012 apparition (Lazzaro et al. 2013).

For the five potential source populations, there are 55 asteroids with available visible spectra from different surveys; these include the SMASS (Bus & Binzel 2002b), the S3 OS2 (Lazzaro et al. 2004), the NEMCASS (the Near-Earth and Mars-Crosser Asteroids Spectroscopic Survey; de León et al. 2010b), and SINEO (Lazzarin et al. 2004, 2005). These populations also have SDSS colors for a significant fraction of their members (Parker et al. 2008). The available spectra and the SDSS colors are sufficiently diagnostic to rule out the Polana family as a likely source of JU₃.

As stated in Section 1, JU₃ has been classified as a Cg-type asteroid in the SMASS classification system, and its near-infrared spectrum (Figure 3) is also consistent with those of C-type asteroids (e.g., DeMeo et al. 2009). Dynamically, the two populations most likely to be the source of JU₃ are the low-inclination and low-albedo background asteroids and the Polana family, in that order. At visible wavelengths, the background contains objects with C-type visible spectra or colors. In contrast, the available visible colors and spectra for the Polana family indicate that B-type objects are most abundant (e.g., Campins et al. 2010; Gayon-Markt et al. 2012).

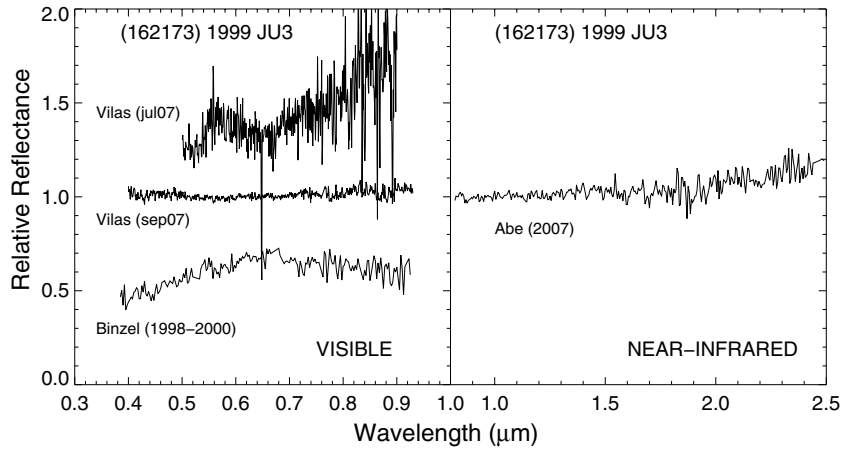


Figure 3. Left panel: the three published reflectance spectra of JU_3 at visible wavelengths (0.4–1.0 μm ; Binzel et al. 2001, Vilas 2008); these three spectra have been offset for clarity. We note that these three spectra of JU_3 are not entirely consistent with each other, so we use the spectrum with highest signal-to-noise (2007 September) for comparison with other asteroids. The right panel shows the only published near-infrared spectrum (0.8–2.4 μm ; Abe et al. 2008). Note the close agreement between the 2007 September visible spectrum and the near-infrared spectrum in the overlap region between 0.8 and 1.0 μm .

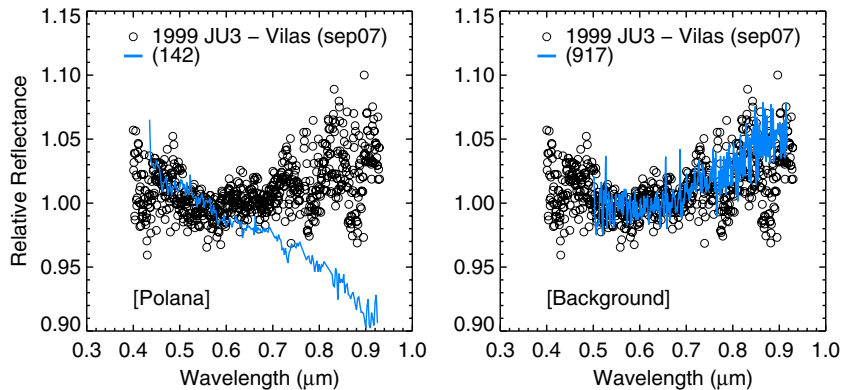


Figure 4. Reflectance spectrum of JU_3 (the spectrum obtained on 2007 September; Vilas 2008) is plotted (open circles) with spectra of two asteroids (blue lines), each from one of the candidate source populations based on purely dynamical arguments: the Polana family and the background. This comparison illustrates how the available spectra and SDSS colors rule out the Polana family as a likely source of JU_3 .

(A color version of this figure is available in the online journal.)

In Figure 4, we illustrate the spectral match between JU_3 and a member of the background (we found more than one good match), asteroid 917 Lyka, and the mismatch with a member of the Polana family, asteroid 142 Polana. So the available spectral and color information favors the background over the Polana family. We note that there is one member of the Polana family with a published C-type spectrum that matches that of JU_3 , asteroid 3999, however, dynamical arguments suggest that this object is an interloper and not a real member of the family. In the case of the Erigone, Clarissa, and Sulamitis families, there is very little spectral information. However, this does not impact our conclusions since the orbital dynamics do not favor any of these three families as sources of JU_3 .

3. CONCLUSIONS

The most likely main belt origin of near-Earth asteroid (162173) 1999 JU_3 are low-albedo and low-inclination asteroids in the inner belt, more specifically the region between 2.15 and 2.5 AU and with inclinations lower than 12° . Within this region, the most likely source population is a background of low-albedo asteroids outside of the four well-defined low-albedo families. This conclusion is based on the following results.

1. The dynamical evidence discussed in Section 2 favors this region with the ν_6 resonance as the strongly preferred

delivery route (100% probability, according to the Bottke et al. 2002 model).

2. The albedo of JU_3 ($p_v = 0.07 \pm 0.01$) narrows potential sources to those with low-albedo. The low-inclination inner belt contains four well-defined low-albedo asteroid families, namely Clarissa, Erigone, Polana, and Sulamitis, and a recently identified background of low-albedo asteroids outside these families.
3. These background asteroids are a collisionally evolved population, which has been and is currently delivering JU_3 -sized objects to the ν_6 resonance. This group appears to deliver several times more objects to this resonance than any of the low-albedo families. In contrast, the Erigone, Clarissa, and Sulamitis families do not contribute large enough objects to the ν_6 resonance (Figure 2).
4. The Polana family is capable of delivering objects the size of JU_3 into the ν_6 resonance, but it contains about half as many kilometer-sized objects as the background population. In addition, the B-type spectra and colors of the Polana family are distinct from those of JU_3 , which has a C-type spectrum (Figure 3).
5. In order for the Yarkovsky effect to move objects from the inner belt into the ν_6 resonance, they have to have retrograde rotation, and the current spin of JU_3 is retrograde.

H.C. acknowledges support from NASA’s Near-Earth Object Observations program and from the National Science Foundation. H.C. was a visiting astronomer at the Observatoire de Paris and at the Observatoire de la Côte d’Azur, in France, funded by a grant from the European Science Foundation’s Gaia Research for European Astronomy Training. H.C. was also a visiting astronomer at the “Instituto de Astrofísica de Canarias” in Tenerife, Spain. J.deL. gratefully acknowledges financial support from the Spanish “Secretaría de Estado de Investigación, Desarrollo e Innovación” (Juan de la Cierva contract). J.L. acknowledges support from the projects AYA2011-29489-C03-02 and AYA2012-39115-C03-03 (MINECO). Part of the data utilized in this publication were obtained and made available by the MITUH-IRTF Joint Campaign for NEO Reconnaissance. The IRTF is operated by the University of Hawaii under Cooperative Agreement No. NCC 5-538 with the National Aeronautics and Space Administration, Office of Space Science, Planetary Astronomy Program. The MIT component of this work is supported by the National Science Foundation under grant No. 0506716.

REFERENCES

- Abe, M., Kawakami, K., Hasegawa, S., et al. 2008, in 39th Lunar and Planetary Science Conference (Houston, Texas: Lunar and Planetary Institute), 1594
- Binzel, R. P., Harris, A. W., Bus, S. J., et al. 2001, *Icar*, 151, 139
- Bottke, W. F., Durda, D. D., Nesvorný, D., et al. 2005, *Icar*, 175, 111
- Bottke, W. F., Morbidelli, A., Jedicke, R., et al. 2002, *Icar*, 156, 399
- Bus, S. J., & Binzel, R. P. 2002a, *Icar*, 158, 146
- Bus, S. J., & Binzel, R. P. 2002b, *Icar*, 158, 106
- Campins, H., Emery, J. P., Kelley, M., et al. 2009, *A&A*, 503, L17
- Campins, H., Morbidelli, A., Tsiganis, K., et al. 2010, *ApJL*, 721, L53
- Cellino, A., Zappalà, V., Doressoundiram, A., et al. 2001, *Icar*, 152, 225
- de León, J., Campins, H., Tsiganis, K., Morbidelli, A., & Licandro, J. 2010a, *A&A*, 513, A26
- de León, J., Licandro, J., Serra-Ricart, M., Pinilla-Alonso, N., & Campins, H. 2010b, *A&A*, 517, A23
- DeMeo, F. E., Binzel, R. P., Slivan, S. M., & Bus, S. J. 2009, *Icar*, 202, 160
- Fujiwara, W., Kawaguchi, J., Yeomans, D. K., et al. 2006, *Sci*, 312, 1330
- Gayon-Markt, J., et al. 2012, *MNRAS*, 424, 508
- Hasegawa, S., Müller, T. G., Kawakami, K., et al. 2008, *PASJ*, 60, S399
- Lazzarin, M., Marchi, S., Barucci, M. A., di Martino, M., & Barbieri, C. 2004, *Icarus*, 169, 373
- Lazzarin, M., Marchi, S., Magrin, S., & Licandro, J. 2005, *MNRAS*, 359, 1575
- Lazzaro, D., Angeli, C. A., Carvano, J. M., et al. 2004, *Icar*, 172, 179
- Lazzaro, D., Barucci, M. A., Perna, D., et al. 2013, *A&A*, 549, L2
- Mainzer, A., Davidson, K., & Ferland, G. J. 2011, *ApJ*, 741, 70
- Masiero, J., Mainzer, A. K., Grav, T., et al. 2011, *ApJ*, 741, 68
- Michel, P., & Delbo, M. 2010, *Icar*, 209, 520
- Morbidelli, A., & Gladman, B. 1998, *M&PS*, 33, 999
- Morbidelli, A., & Nesvorný, D. 1999, *Icar*, 139, 295
- Müller, T. G., Durech, J., Hasegawa, S., et al. 2011, *A&A*, A525, A145
- Nesvorný, D. 2010, Nesvorný HCM Asteroid Families V1.0, EAR-A-VARGBDET-5-NESVORNYFAM-V1.0, NASA Planetary Data System
- Parker, A., Ivezić, Ž., Jurić, M., et al. 2008, *Icar*, 198, 138
- Pinilla-Alonso, N., Lorenzi, V., Campins, H., de Leon, J., & Licandro, J. 2013, *A&A*, 552, A79
- Tholen, D. J., & Barucci, M. A. 1989, in Asteroids II, ed. R. P. Binzel, T. Gehrels, & M. S. Matthews (Tucson, AZ: Univ. Arizona Press), 298
- Vilas, F. 2008, *AJ*, 135, 1101
- Vokrouhlický, D., Brož, M., Bottke, W. F., Nesvorný, D., & Morbidelli, A. 2006, *Icar*, 182, 118
- Walsh, K. J., et al. 2013, *Icar*, in press